

1 **Influence of multi-walled carbon nanotubes on the microbial biomass, enzyme activity,**  
2 **and bacterial community structure in 2,4-dichlorophenol-contaminated sediment**

3

4 Biao Song<sup>a,b</sup>, Jilai Gong<sup>a,b</sup>, Wangwang Tang<sup>a,b</sup>, Guangming Zeng<sup>a,b,\*</sup>, Ming Chen<sup>a,b</sup>, Piao Xu<sup>a,b</sup>,

5 Maocai Shen<sup>a,b</sup>, Shujing Ye<sup>a,b</sup>, Haopeng Feng<sup>a,b</sup>, Chengyun Zhou<sup>a,b</sup>, Yang Yang<sup>a,b</sup>

6

7 <sup>a</sup> College of Environmental Science and Engineering, Hunan University, Changsha 410082,

8 PR China

9 <sup>b</sup> Key Laboratory of Environmental Biology and Pollution Control (Hunan University),

10 Ministry of Education, Changsha 410082, PR China

11

12 \* Corresponding author at: College of Environmental Science and Engineering, Hunan

13 University, Changsha 410082, PR China

14 E-mail addresses: [zgming@hnu.edu.cn](mailto:zgming@hnu.edu.cn) (G. Zeng).

15

ACCEPTED MS

16 **Abstract**

17 The rise in manufacture and use of carbon nanotubes has aroused the concern  
18 about their potential risks associated with coexisting pollutants in the aquatic  
19 environment. 2,4-dichlorophenol (2,4-DCP), with a high toxicity to many aquatic  
20 organisms, is a widespread pollutant resulting from the extensive use of pesticides and  
21 preservatives. In this article, the adsorption of 2,4-DCP by riverine sediment and the  
22 responses of sediment microbial community to 2,4-DCP were studied in the presence  
23 of multi-walled carbon nanotubes (MWCNTs). Adding MWCNTs significantly  
24 increased the adsorption amount of sediment for 2,4-DCP from 0.541 to 1.44 mg/g as  
25 the MWCNT concentration increased from 0 to 15 mg/g. The responses of sediment  
26 microbial community were determined after one-month exposure to MWCNTs at  
27 different concentrations (0.05, 0.5, 5, and 50 mg/g). The microbial biomass carbon in  
28 the sediment contaminated with 2,4-DCP increased in the presence of 5 mg/g of  
29 MWCNTs (from 0.06 to 0.1 mg/g), but not significantly changed at other MWCNT  
30 concentrations. For the sediments contaminated with 2,4-DCP, the presence of  
31 MWCNTs made no difference to urease activity, while the dehydrogenase activity  
32 slightly increased with the addition of 5 mg/g of MWCNTs and decreased in the  
33 presence of 50 mg/g of MWCNTs. The changes of sediment bacterial communities  
34 were further determined by 16S rRNA gene sequencing. Based on the weighted  
35 UniFrac distance between communities, the clustering analysis suggested that the  
36 contamination of 2,4-DCP affected the bacterial community structure in a greater  
37 degree than that caused by MWCNTs at relatively low concentrations ( $\leq 5$  mg/g).

38 *Bacteroidetes*, *Planctomycetes*, and *Nitrospirae* were feature bacterial phyla to reflect  
39 the effects of MWCNTs and 2,4-DCP on sediment bacterial community. These results  
40 may contribute to the understanding of microbial community response to co-exposure  
41 of MWCNTs and 2,4-DCP and the assessment of associated ecological risks.

42

43 **Keywords:** Carbon nanotubes; Microbial community; Sediment; 2,4-dichlorophenol;  
44 16S rRNA gene

45

Accepted MS

## 46 1. Introduction

47 As a kind of one-dimensional nanomaterials with many attractive properties,  
48 carbon nanotubes (CNTs) have been widely studied and applied in various fields, such  
49 as composites, microelectronics, medicine, energy, and environment (Schnorr and  
50 Swager 2011, Song et al. 2018a). Currently, global production capacity of CNTs has  
51 reached thousands of tons per year, and the global market is \$3.95 billion in 2017 and  
52 expected to rise to \$9.84 billion by 2023 (Tamez Ramírez and Vega-Cantú 2019).  
53 According to the layer number of tube walls, CNTs are divided into single-walled  
54 CNTs (SWCNTs) and multi-walled CNTs (MWCNTs). MWCNTs are preferred in  
55 industrial applications due to their lower cost, which makes them the majority of  
56 current CNT market (Zhai et al. 2016, Bishop et al. 2017). Mass manufacture and use  
57 of CNTs will certainly result in their release into the environment, as CNTs can enter  
58 into the environment during the whole product life cycle including manufacturing,  
59 processing, service stage, recycling, and disposal (Köhler et al. 2008). Most of the  
60 released CNTs will eventually enter into the natural waters and accumulate in  
61 sediments (Liu and Cohen 2014). The predicted concentrations of CNTs in Europe  
62 soil, sludge treated soil, and sediment were 1.51, 73.6, and 241 ng/kg/y, respectively  
63 (Gottschalk et al. 2009). According to the simulation by Koelmans et al. (2009), the  
64 total concentration of manufactured carbon-based nanoparticles in aquatic sediment  
65 was 1.2–2000 µg/kg, and the CNT concentration might reach a higher level in the  
66 future. This has aroused concern about the potential risks of CNTs in the aquatic  
67 environment.

68 Due to the nanoscale radial dimension and unique microstructure, CNTs can  
69 cause toxic effects on fish, invertebrates, algae, and microorganisms in the aquatic  
70 environment (Chen et al. 2018). Additionally, CNTs may interact with coexisting  
71 pollutants and change their mobility, toxicity, and bioavailability, especially for  
72 hydrophobic organic pollutants with aromatic rings (Myer et al. 2017, Song et al.  
73 2017a, Fan et al. 2018, Song et al. 2018b). This kind of pollutants can be strongly  
74 adsorbed by CNTs via hydrophobic interaction and  $\pi$ - $\pi$  interaction between the  
75 aromatic rings of organic compounds and the highly polarizable graphene sheets of  
76 CNTs (Jesionowski et al. 2014). Our previous study showed that incorporating 0.5%,  
77 1.0%, and 1.5% (w/w) MWCNTs into riverine sediment significantly increased the  
78 adsorption capacity of sediment for sodium dodecyl benzene sulfonate and impeded  
79 its transport through the sediment column (Song et al. 2018b). Fan et al. (2018)  
80 found that 50 mg/L of MWCNTs could decrease the toxicity and bioavailability of  
81 paraquat (0.82 mg/L) to *Arabidopsis thaliana*, and the protective effect on root  
82 surface area against paraquat toxicity was attributed to the adsorption of paraquat by  
83 MWCNTs. Although many valuable results have been obtained, efforts are still  
84 required to advance the understanding of environmental risks of CNTs.

85 Sediment microbial communities are vital to maintaining the health and services  
86 of aquatic ecosystems (Song et al. 2018b, Orland et al. 2019). Compared with fish,  
87 invertebrates, and algae, sediment microbial communities are more likely to be  
88 exposed to CNTs and pollutants in sediment as microorganisms are virtually present  
89 in all sediment environments. The interactions among CNTs, pollutants, and

90 microbial communities should be studied for a better assessment of the ecological  
91 risks of CNTs (Xie et al. 2016, Song et al. 2017b). As an important industrial  
92 material, 2,4-dichlorophenol (2,4-DCP) is extensively used for manufacturing  
93 pesticides (e.g., 2,4-dichlorophenoxyacetic acid, oxadiazon, and nitrofen), medicines  
94 (e.g., bithionol), and preservatives (e.g., triclosan). The occurrence of 2,4-DCP in  
95 aquatic environment mainly arises from the widespread use of pesticides and the  
96 wastewater discharge from related industrial activities (Zhou et al. 2017). In the  
97 surface water of China, the concentrations of 2,4-DCP were reported ranging from <  
98 1.1 to 19,960 ng/L (Gao et al. 2008). Exposure to 2,4-DCP can cause pernicious  
99 effects to many aquatic organisms, such as oxidative damage to *Daphnia magna* (Wu  
100 et al. 2011), growth inhibition to algae (Ertürker and Saçan 2012), and DNA damage in  
101 fish (Huang et al. 2018), and even cause human health risks via food and drinking  
102 water (Igbinoso et al. 2013). It is significant to understand the ecological risks of  
103 2,4-DCP. To our knowledge, there are few studies about the interactions among  
104 CNTs, 2,4-DCP, and microbial communities in sediment. In this research, MWCNTs  
105 were added to 2,4-DCP-contaminated sediment at the concentrations of 0.05, 0.5, 5,  
106 and 50 mg/g, and microbial community in the sediment was analyzed after  
107 one-month exposure. These MWCNT concentrations were chosen to match those  
108 used in previous related studies (Chung et al. 2011, Kerfahi et al. 2015), and the  
109 extremely high concentration of MWCNTs (50 mg/g) was considered a worst case of  
110 accidental spills or CNT waste accumulation (Shrestha et al. 2013). The main  
111 purpose of this study is to assess the impacts of MWCNTs on the microbial biomass

112 carbon, enzyme activity, and bacterial community structure in  
113 2,4-DCP-contaminated riverine sediment. It is expected that this study would  
114 promote the understanding of ecological impacts of CNTs and associated risks.

115

## 116 **2. Materials and methods**

### 117 *2.1. Sediment and MWCNTs*

118 Sediment was collected from Changsha section of the Xiangjiang River, the  
119 largest river in Hunan Province of China. Prior to use, the sediment was air-dried,  
120 crushed, ground, sieved to less than one mm, and manually homogenized. The  
121 contaminated sediment was prepared by spiking 2,4-DCP with the following  
122 procedures. Firstly, 2,4-DCP was first dissolved in  $\text{CH}_2\text{Cl}_2$  and mixed with 25% (by  
123 weight) of the total sediment. For evaporating the solvent completely, the mixture was  
124 stirred every 15 min. Then, the treated sediment was mixed with the rest 75% of  
125 sediment. After manual homogenization, 50% (v/w) ultrapure water was added to  
126 adjust the moisture content of spiked sediment. The final concentration of 2,4-DCP in  
127 the spiked sediment was 30 mg/kg. The 2,4-DCP concentration for treatment was  
128 decided at this level based on the consideration of both the environmental  
129 concentration of chlorophenol and the experimental concentrations used in previous  
130 related studies (Khairy 2013, Zhou et al. 2013, Dallinger and Horn 2014, Zhou et al.  
131 2017). MWCNTs were bought from Chengdu Organic Chemistry Co., China.  
132 According to the technical data provided by the manufacturer, the CNT content,  
133 length, and outer diameter of MWCNTs are > 90%, 5–20  $\mu\text{m}$ , and 10–20 nm,

134 respectively. There are some impurities of Fe and O in the MWCNTs, and the C  
135 content is > 95%. The microstructures of MWCNTs and sediment were characterized  
136 by scanning electron microscope (SEM, Fig. S1). The determined pH value and  
137 organic carbon content of sediment were 7.92 and 1.63% (w/w), respectively.  
138 Sediment elemental composition was analyzed by energy disperse spectroscopy  
139 (EDS), and O, Si, Al, Fe, C, and K were the main component elements (Fig. S1e).

140

## 141 2.2. Adsorption experiments

142 The adsorption experiments were performed in conical flasks containing  
143 2,4-DCP solutions of various concentrations (from 10–80 mg/L), using MWCNTs,  
144 sediment, and sediment-MWCNT mixtures as adsorbents. The 2,4-DCP solutions  
145 were made through diluting the stock solution of 2,4-DCP dissolved in methanol. For  
146 minimizing the cosolvent effects, methanol concentrations in the prepared 2,4-DCP  
147 solutions were controlled below 0.1% (v/v) (Wang et al. 2014). The adsorbent dosage  
148 of MWCNTs was 0.3 g/L and the dosages of sediment and sediment-MWCNT  
149 mixtures were both 20 g/L. The MWCNT concentration in the sediment-MWCNT  
150 mixtures was 0.05, 0.5, 5, and 50 mg/g, respectively. These conical flasks were  
151 shaken at 180 rpm and  $25 \pm 1$  °C for 24 h, followed by static settlement of the  
152 adsorbents for 6 h. The concentrations of 2,4-DCP in the supernatant were measured  
153 by high performance liquid chromatography (HPLC, Agilent 1100, USA) equipped  
154 with a reversed-phase C18 column and a variable wavelength detector. Methanol  
155 solution (70%, v/v) was used as the mobile phase with a flow rate of 1 mL/min. The

156 detection wavelength was 284 nm.

157

### 158 *2.3. Experimental design for MWCNT exposure*

159 Ten treatments in triplicate were implemented to investigate the impacts of  
160 MWCNTs on microbial community in riverine sediment contaminated with 2,4-DCP  
161 (detailed experimental design is displayed in Table S1 of the Supplementary Material).  
162 MWCNT powders were added to the uncontaminated and contaminated sediments at  
163 the concentrations of 0 (T1 and T2), 0.05 (T3 and T4), 0.5 (T5 and T6), 5 (T7 and T8),  
164 and 50 mg/g (T9 and T10), respectively. The MWCNT-sediment mixtures were  
165 manually homogenized. The sediment moisture was kept at 50% (v/w) and adjusted  
166 daily. A month later, samples were taken out for the subsequent tests.

167

### 168 *2.4. Measurement of microbial biomass and enzyme activity*

169 Microbial biomass carbon was measured by fumigation-extraction method (Deng  
170 et al. 2016). Specifically, 12.5 g of sediment were fumigated with ethanol-free  
171 chloroform at 25 °C for 24 h to lyse microbial cells and release cellular content. After  
172 removing the chloroform, the sediment was transferred to a conical flask and 50 mL  
173 of 0.5 M K<sub>2</sub>SO<sub>4</sub> extractant were added. The mixture was shaken for 30 min before  
174 centrifugal treatment. Subsequently, the supernatant was filtered and the total organic  
175 carbon in filtrate was determined by a total organic carbon analyzer. Another 12.5 g of  
176 sediment without fumigation were used as the control, following the same extraction  
177 procedure.

178 Urease activity was quantified by the amount of  $\text{NH}_4^+$  produced from  
179 urease-mediated urea hydrolysis within a certain reaction time, and the concentration  
180 of  $\text{NH}_4^+$  was measured by the indophenol blue colorimetric method (Liu et al. 2018).  
181 Specifically, 0.5 mL toluene was added to 1 g of sediment in a centrifuge tube. After  
182 15 min, 2.5 mL of 10% urea solution and 5 mL of citrate buffer solution (pH 6.7)  
183 were added. The sample tube was then incubated at 37 °C for 24 h. After that, the  
184 mixture was centrifuged, and the supernatant was collected and diluted 10 times with  
185 ultrapure water. Subsequently, 4 mL of the diluted supernatant was moved to another  
186 centrifuge tube, and 0.8 mL of 1.35 M sodium phenate solution and 0.6 mL of sodium  
187 hypochlorite solution (active chlorine 0.9%) were added. After 20 min, the mixture  
188 was diluted with ultrapure water to a final volume of 10 mL and the absorbance at 578  
189 nm was recorded. The same procedures without urea substrate (using ultrapure water  
190 instead of urea solution) were conducted on another 1 g of sediment as the control.

191 Dehydrogenase activity was measured by a reduction reaction using  
192 2,3,5-triphenyl tetrazolium chloride (TTC) as the hydrogen acceptor, and quantified  
193 by the amount of generated red 2,3,5-triphenyl formazan (TF) by colorimetric method  
194 (Mierzwa-Hersztek et al. 2016). Specifically, 2 mL of 1% TTC solution, 2 mL of  
195 Tris-HCl buffer solution (pH 7.6), and 2 mL of ultrapure water were added to 1.5 g of  
196 sediment. Then, the mixture was incubated at 37 °C for 6 h, and the formed TF was  
197 extracted by 5 mL of methanol. After filtration, the absorbance at 485 nm was  
198 measured. The same procedures without the addition of TTC (using ultrapure water  
199 instead of TTC solution) were performed on another 1.5 g of sediment as the control.

200

## 201 2.5. DNA extraction and 16S rRNA gene sequencing

202 Microbial genomic DNA was extracted from 200 mg of sediment using the  
203 Mag-Bind<sup>®</sup> Environmental DNA Kit (Omega Bio-tek, Norcross, GA, USA) according  
204 to the protocol provided by the manufacturer. The integrity of extracted DNA was  
205 checked by agarose gel electrophoresis. Subsequently, the genomic DNA was  
206 accurately quantified for polymerase chain reaction (PCR) with the Qubit<sup>™</sup> ssDNA  
207 Assay Kit in a Qubit<sup>™</sup> 3.0 fluorometer (Thermo Fisher Scientific, Waltham, MA,  
208 USA). The hypervariable V3-V4 region of bacterial 16S rRNA genes was amplified  
209 by nested PCR with the primer 341F (5'-CCTACGGGNGGCWGCAG-3') and 805R  
210 (5'-GACTACHVGGGTATCTAATCC-3') (Zhang et al. 2018). The PCR products  
211 were separated by agarose gel electrophoresis, and the DNA was purified and  
212 recovered with *MagicPure*<sup>™</sup> DNA Spin Selection beads (TransGen Biotech Co.,  
213 Beijing, China). The recovered DNA was accurately quantified prior to the 16S rRNA  
214 gene sequencing, and 20 µmol samples were used for the sequencing by an Illumina  
215 MiSeq platform (Illumina, San Diego, CA, USA).

216

## 217 2.6. Data analysis

218 The results of adsorption experiments were fitted by Langmuir and Freundlich  
219 isotherm models to analyze the effects of MWCNTs on the adsorption of 2,4-DCP by  
220 sediment (detailed description of the two models is shown in the Supplementary  
221 Material).

222 Microbial biomass carbon (mg/g) was calculated with the following equation:

$$223 \text{ Microbial biomass } C = \frac{(C_{f+} - C_{f-}) \times V}{0.45 \times m} \quad (1)$$

224 where  $C_{f+}$  (mg/L) and  $C_{f-}$  (mg/L) are the concentrations of total organic carbon  
225 measured from the sediments with and without fumigation,  $V$  (L) is the extract  
226 volume,  $m$  (g) is the sediment weight, and 0.45 is a conversion factor (Deng et al.  
227 2016). The difference value calculation of total organic carbon can eliminate the  
228 possible influence of MWCNTs on the measurement of microbial biomass carbon.

229 Urease activity ( $\mu\text{g NH}_4^+$ /g/h) was calculated according to the following equation:

$$230 \text{ Urease activity} = \frac{(C_{u+} - C_{u-}) \times V_3 \times V_1 \times n}{T \times m \times V_2} \quad (2)$$

231 where  $C_{u+}$  ( $\mu\text{g/L}$ ) and  $C_{u-}$  ( $\mu\text{g/L}$ ) are the concentration of  $\text{NH}_4^+$  measured with and  
232 without urea substrate,  $V_1$  (L) is the total extract volume,  $V_2$  (L) is the volume of  
233 diluted supernatant for colorimetric test,  $V_3$  (L) is the final volume of colored solution,  
234  $m$  (g) is the sediment weight,  $n$  is the dilution ratio, and  $T$  (h) is the incubation time.

235 Dehydrogenase activity ( $\mu\text{g TTC/g/h}$ ) was calculated with the following equation:

$$236 \text{ Dehydrogenase activity} = \frac{(C_{T+} - C_{T-}) \times V}{T \times m} \quad (3)$$

237 where  $C_{T+}$  ( $\mu\text{g/L}$ ) and  $C_{T-}$  ( $\mu\text{g/L}$ ) are the concentrations of TTC measured with and  
238 without the addition of TTC,  $V$  (L) is the extract volume,  $m$  (g) is the sediment weight,  
239 and  $T$  (h) is the incubation time. Analysis of variance (ANOVA) was carried out to  
240 determine the differences between group mean values, and a P-value less than 0.05  
241 suggests a statistically significant difference.

242 Sequenced reads were clustered into different operation taxonomic units (OTUs)  
243 at a similarity level of 97%. The corresponding taxonomic information was obtained

244 using the Ribosomal Database Project Classifier (Wang et al. 2007).

245 The  $\beta$ -diversity differences between different treatments were quantified using  
246 the unique fraction metric (UniFrac) (Lozupone et al. 2011). The weighted UniFrac  
247 distance that takes into account the difference in proportional abundance of the taxa  
248 between two samples was calculated based on a phylogenetic tree generated by  
249 FastTree using maximum likelihood method (Price et al. 2010). The values of  
250 weighted UniFrac distance range from zero to one, and a smaller distance indicates a  
251 more similar phylogenetic structure between two communities.

252 Linear discriminant analysis (LDA) effect size (LEfSe) method was used to  
253 determine the feature taxa most likely to explain the differences between different  
254 treatments. LEfSe couples the factorial Kruskal-Wallis test for statistical significance  
255 with the pairwise Wilcoxon test for biological consistency, and the discriminative  
256 features are ranked by effect size based on LDA (Segata et al. 2011). In the LEfSe  
257 analysis of this study, the  $\alpha$  values for the factorial Kruskal-Wallis test among classes  
258 and the pairwise Wilcoxon test between subclasses were both 0.05, and the  
259 non-negative threshold on the logarithmic LDA score for discriminative features was  
260 3.5.

261

### 262 **3. Results and discussion**

263

#### 264 *3.1. Effects of MWCNTs on the adsorption of 2,4-DCP by sediment*

265 The presence of MWCNTs in sediment significantly affected the adsorption of

266 2,4-DCP by sediment. Measured and fitted isotherms of 2,4-DCP adsorption by  
267 MWCNTs, sediment, and sediment-MWCNT mixtures are illustrated in Fig. 1. Fitting  
268 parameters of the Langmuir model and the Freundlich model are displayed in Table 1.  
269 Both the two models showed a good fitting effect to the results with a minimum  
270  $R^2$ -value of 0.944. According to the estimated values of  $q_m$  and  $K_F$ , there were about  
271 two orders of magnitude difference between MWCNTs and sediment in the adsorption  
272 amount for 2,4-DCP. The maximum adsorption amount of MWCNTs was 47.6 mg/g,  
273 while that of sediment was only 0.541 mg/g. This result can be explained by the  
274 strong interactions between MWCNTs and 2,4-DCP. On the one hand, the  
275 hydrophobic nature of both MWCNTs and 2,4-DCP made them easily aggregated in  
276 aqueous solution through hydrophobic interaction (Kragulj et al. 2015). On the other  
277 hand, the  $\pi$ - $\pi$  stacking between the benzene ring of 2,4-DCP and the graphene sheets  
278 of MWCNTs further enhanced the adsorption (Apul and Karanfil 2015).

279 After the incorporation of MWCNTs, the adsorption capacity of sediment for  
280 2,4-DCP significantly increased ( $P = 0.003$ ). Compared with the pure sediment, the  
281 sediment with 5, 10, and 15 mg/g of MWCNTs showed a 0.85-fold, 1.18-fold, and  
282 1.66-fold increase in the  $q_m$  value, respectively (Table 1). This phenomenon generally  
283 occurs when CNTs show high adsorption capacity for pollutant while the interaction  
284 between sediment and pollutant is relatively weak. Based on the adsorption  
285 experiments, biota-sediment accumulation factor (BSAF) for 2,4-DCP in sediments  
286 with different concentration of MWCNTs was estimated (Table S2). BSAF is widely  
287 used for assessing the risk of pollutant accumulation by biotas from sediment (Shen et

288 al. 2018). The estimated BSAF decreased from 31.8 to 6.6 with the increasing  
289 MWCNT concentration in sediment. This result indicates a lower bioavailability and  
290 biodegradation of 2,4-DCP in sediment in the presence of MWCNTs. In a previously  
291 reported study, Zhou et al. (2013) found that CNTs could inhibit the 2,4-DCP  
292 degradation and mineralization in soil, as the adsorption of 2,4-DCP by CNTs  
293 decreased the bioavailability of 2,4-DCP. Additionally, CNTs and 2,4-DCP might  
294 produce combined effects on the sediment microorganisms. Therefore, the effects of  
295 MWCNTs on microbial biomass, enzyme activity, and bacterial community structure  
296 in the sediment contaminated with 2,4-DCP were further studied.

### 298 3.2. Effects of MWCNTs on the microbial biomass and enzyme activity

299 The changes in microbial biomass carbon of the sediments from different  
300 treatments are presented in Fig. 2a. For the sediments uncontaminated with 2,4-DCP,  
301 the microbial biomass carbon significantly decreased from 0.23 to 0.18 and 0.09 mg/g  
302 in the presence of 5 and 50 mg/g of MWCNTs, respectively. This result was  
303 consistent with previously reported findings that high concentrations of MWCNTs ( $\geq$   
304 5 mg/g) could cause an obvious decrease in the microbial biomass carbon of soil  
305 (Chung et al. 2011, Shrestha et al. 2013). The antibacterial property of MWCNTs  
306 could be accounted for this phenomenon. When a large number of MWCNTs were  
307 added into the sediment, microbes might be wrapped by long MWCNTs, which  
308 resulted in the isolation of microbes from the external environment and their growth  
309 inhibition (Smith and Rodrigues 2015). Additionally, the sharp ends of short

310 MWCNTs might pierce the cell membrane, and lead to severe damage to the microbes  
311 (Song et al. 2018a). The toxicity of 2,4-DCP decreased the microbial biomass carbon  
312 in a condition of the same MWCNT concentration. Compared with the sediment  
313 contaminated with only 2,4-DCP (T2), the addition of 0.05, 0.5, and 50 mg/g of  
314 MWCNTs had no significant effects on the microbial biomass carbon, while that  
315 increased from 0.06 to 0.11 mg/g in the presence of 5 mg/g of MWCNTs. The  
316 increased microbial biomass carbon might result from the decreased toxicity of  
317 2,4-DCP due to the adsorption by MWCNTs, but the effect was lost with higher  
318 concentration of MWCNTs as a result of the significant antibacterial effect caused by  
319 a large number of MWCNTs (Song et al. 2019).

320 Urease is an important extracellular enzyme for nitrogen mineralization and it is  
321 widely used for assessing the nutrient cycling and microbial nutrient demand  
322 (Cordero et al. 2019). The sediment urease activity in different treatments is  
323 illustrated in Fig. 2b. The sediments uncontaminated with 2,4-DCP exhibited higher  
324 urease activity than that of contaminated sediments, which indicates the inhibiting  
325 effect of 2,4-DCP to the sediment urease. According to a study by Bello et al. (2013),  
326 soil urease activity comes from two main sources: the enzymes produced by active  
327 organisms, and the enzymes stabilized by soil colloids. Therefore, in this study, the  
328 decreased urease activity might be because the toxic effect of 2,4-DCP on microbes  
329 inhibited the activity of urease produced by active organisms. Besides, no significant  
330 difference in the urease activity was found between the sediments contaminated with  
331 2,4-DCP (T2, T4, T6, T8, and T10), suggesting the relative stability of urease

332 stabilized by sediment colloids. For the sediments uncontaminated with 2,4-DCP,  
333 adding 5 mg/g of MWCNTs increased the urease activity from 5.0 to 6.6  $\mu\text{g NH}_4^+/\text{g/h}$ ,  
334 while no significant differences were found between the other treatments. The  
335 stabilizing effect of 5 mg/g of MWCNTs for the free urease released by active  
336 organisms could be the cause, as the adverse effect of MWCNTs at that concentration  
337 on microbes might not be very large and MWCNTs could stabilize the urease via  
338 physical adsorption (Feng and Ji 2011, Jesionowski et al. 2014).

339 Dehydrogenase meaningfully participates in pollutant degradation, organic  
340 matter transformation, and microbial metabolism, which enables it to be widely used  
341 for studying the changes of microbial oxidative activity in contaminated sites (Tan et  
342 al. 2017b). The sediments contaminated with 2,4-DCP showed a slightly higher  
343 dehydrogenase activity than that of uncontaminated sediments, but the differences  
344 were not significant. Compared with the sediments without MWCNTs (T1 and T2),  
345 the dehydrogenase activity of sediment with 5 mg/g of MWCNTs slightly increased,  
346 while the dehydrogenase activity slightly decreased in the presence of 50 mg/g of  
347 MWCNTs. A significant difference in dehydrogenase activity was found between the  
348 sediments containing 5 and 50 mg/g of MWCNTs. The increased dehydrogenase  
349 activity might result from higher metabolic activity due to higher energy consumption  
350 of microbes to resist the MWCNT stress (Tan et al. 2017a), while the evident  
351 antibacterial effect of 50 mg/g of MWCNTs decreased the dehydrogenase activity  
352 (Chung et al. 2011). These results indicate that MWCNTs could have a direct impact  
353 on microbes and thus affect the enzymes they produce. Though the important roles of

354 microbial community in aquatic ecosystems are well acknowledged and understood,  
355 the risk assessment of MWCNTs about their effects on the sediment microbial  
356 community is lacking. The changes of microbial biomass carbon and enzyme activity  
357 may provide valuable information about the potential impact of MWCNTs on the  
358 whole ecosystem, especially under the stress of both MWCNTs and coexisting  
359 pollutants. A two-way ANOVA was further conducted to determine the main effects of  
360 MWCNTs and 2,4-DCP and their interactive effects (Table S3). The results reveal that  
361 both the main effects of MWCNTs and 2,4-DCP and their interactive effects on the  
362 microbial biomass carbon were significant ( $P \leq 0.001$ ). No significant main effect of  
363 MWCNTs on the urease activity ( $P = 0.248$ ) was found, while there was significant  
364 main effect of 2,4-DCP on the urease activity ( $P < 0.001$ ). For the dehydrogenase  
365 activity, significant main effect of MWCNTs ( $P = 0.020$ ) was found. The interaction  
366 between MWCNTs and 2,4-DCP showed no significant effect on neither the urease  
367 activity ( $P = 0.148$ ) nor the dehydrogenase activity ( $P = 0.933$ ). However, the  
368 microbial community structure may not change in a consistent manner with the  
369 enzyme activity (ecological function), as four different outcomes are possible in  
370 microbial community studies: (1) both structure and function change; (2) neither  
371 structure nor function is affected; (3) only structure is altered; and (4) only function  
372 varies (Frossard et al. 2012). Therefore, the bacterial community structure in  
373 sediments of different treatments was further analyzed.

374

375 3.3. Effects of MWCNTs on the bacterial community structure

376 The bacterial community structure at phylum level is shown in Fig. 3a.  
377 *Proteobacteria*, *Bacteroidetes*, and *Firmicutes* were the dominant species in  
378 sediments, and they accounted for 69%–88% of the total bacterial abundance. High  
379 relative abundance of *Proteobacteria* was observed for most treatments, and its  
380 maximum proportion (59%) was found in the sediment with 50 mg/g of MWCNTs  
381 (T10). In the sediment uncontaminated with 2,4-DCP (T1), the relative abundance of  
382 *Bacteroidetes* (36%) was much higher than that of *Firmicutes* (1%) while an opposite  
383 situation in the relative abundance of these two species was found in the sediment  
384 contaminated with 2,4-DCP (T2). The incorporation of MWCNTs affected the relative  
385 abundance of bacterial community structure and it became similar between the  
386 sediments uncontaminated and contaminated with 2,4-DCP when the MWCNT  
387 concentration was extremely high (T9 and T10). A more detailed classification of the  
388 community at class level is illustrated in Fig. 3b. *Sphingobacteriia* and *Clostridia*  
389 were the main classes of *Bacteroidetes* and *Firmicutes*, respectively. *Proteobacteria*,  
390 *Bacteroidetes*, and *Firmicutes* are common bacterial species in the natural sediments  
391 (Zhu et al. 2013). *Proteobacteria* is the largest bacterial phylum with the most diverse  
392 phenotypes, and usually predominates in freshwater sediment (Cheng et al. 2014).  
393 *Bacteroidetes* and *Firmicutes* are more widely studied in gut microbiota, and  
394 *Firmicutes/Bacteroidetes* ratio has been used as an indicator of obesity due to its high  
395 correlation with body mass index and the competitive interaction between the two  
396 species (Koliada et al. 2017). In this study, obvious competitive relationship between

397 *Bacteroidetes* and *Firmicutes* was also observed, and *Firmicutes* was more dominant  
398 than *Bacteroidetes* in T2, T4, T9, and T10. The following reasons might account for  
399 this. On the one hand, many species of *Firmicutes* can participate in the anaerobic  
400 dechlorinating processes of chlorinated organic compounds and utilize them to  
401 proliferate (Zhang et al. 2015), but the activity was restricted in the presence of 0.5  
402 and 5 mg/g of MWCNTs as the bioavailability of 2,4-DCP decreased due to the  
403 adsorption by MWCNTs. On the other hand, *Firmicutes* can form endospores against  
404 various environmental stresses (e.g., lack of nutrients, and toxicity of pollutants)  
405 while *Bacteroidetes* cannot, which makes *Bacteroidetes* more vulnerable to the  
406 pollutant toxicity (Fajardo et al. 2019). Additionally, the alpha diversity (including the  
407 Chao1 index and the Shannon index) of different sediment samples was analyzed to  
408 show the bacterial richness and diversity (Table S4). The 2,4-DCP-contaminated  
409 sediments showed higher species diversity, which might be due to the greater  
410 environmental heterogeneity (Curd et al. 2018).

411 The bacterial community differences between various treatments were quantified  
412 using weighted UniFrac distance, which has been widely used for describing the  
413 diversity differences between communities from different habitats (Lozupone et al.  
414 2011). Based on the weighted UniFrac distance, all treatments were clustered into  
415 three groups (Cluster I–III in Fig. 4). Each of these groups has a distinct sediment  
416 characteristic: uncontaminated with 2,4-DCP (Cluster I), contaminated with 2,4-DCP  
417 (Cluster II), and containing MWCNTs at extremely high concentration (Cluster III).  
418 The high value of weighted UniFrac distance between Cluster I and II showed that the

419 contamination of 2,4-DCP affected the bacterial community structure and the impact  
420 was greater than that caused by 0.05, 0.5, and 5 mg/g of MWCNTs. The bacterial  
421 community structure in sediments uncontaminated and contaminated with 2,4-DCP  
422 became similar in the presence of 50 mg/g of MWCNTs (T9 and T10) and these two  
423 treatments were grouped into a separate cluster, indicating that the bacterial  
424 community was mainly influenced by MWCNTs rather than 2,4-DCP in that case.  
425 Additionally, the dissimilarity of bacterial community structure within Cluster II (a  
426 maximum weighted UniFrac distance of 0.392) was greater than that within Cluster I  
427 (a maximum weighted UniFrac distance of 0.241), which suggests that adding 0.5 or 5  
428 mg/g of MWCNTs made a greater difference to the bacterial community in sediments  
429 contaminated with 2,4-DCP than that of uncontaminated sediments. This might be  
430 because MWCNTs at those concentration levels effectively adsorbed 2,4-DCP and  
431 reduced its toxicity and bioavailability to bacteria.

432 LEfSe is a widely used tool for high-dimensional biomarker discovery and  
433 explanation, and LEfSe algorithm was performed to further identify feature taxa in the  
434 three clusters (Segata et al. 2011). In this study, this tool was used to find feature  
435 bacteria in each cluster and determine their contributions to the differences between  
436 groups. The contributions were indicated by the logarithmic LDA score of significant  
437 different taxa (Fig. S2). The phylum *Bacteroidetes*, the genus *Sporacetigenium*, and  
438 the genus *Symbiobacterium* were feature bacterial taxa with the highest logarithmic  
439 LDA score in Cluster I, II, and III, respectively. However, these three taxa were not at  
440 the same classification level. Therefore, a cladogram that showed all significantly

441 different taxa at different classification level was plotted and displayed in Fig. 5. It  
442 was found that *Bacteroidetes* (log LDA score = 5.27), *Planctomycetes* (log LDA score  
443 = 4.13), and *Nitrospirae* (log LDA score = 3.93) were feature bacterial phyla in  
444 Cluster I, II, and III, respectively. Additionally, the corresponding branches showed  
445 significantly different taxa from genus to phylum level, which indicates the  
446 importance of these three phyla in distinguishing the differences between groups.  
447 Relative abundance of the three feature phyla in different groups was illustrated in Fig.  
448 S3. As a common species in the natural sediments, *Bacteroidetes* showed relatively  
449 high abundance in Cluster I, and were more vulnerable to the toxicity of 2,4-DCP and  
450 high concentration of MWCNTs, which makes them a sensitive biological indicator  
451 (Wolińska et al. 2017). *Planctomycetes* are a distinct group of bacteria that are  
452 widespread in the aquatic environment, and may be potential candidates for sediment  
453 quality assessment as this bacterial species show different dose-response behaviour to  
454 different pollutants (Flores et al. 2014). *Nitrospirae* play important roles in biological  
455 nitrification and nitrogen cycle, and similar result of the increase in relative  
456 abundance of *Nitrospirae* after CNT exposure was also reported in a previous study  
457 (Qian et al. 2018), which supports *Nitrospirae* as a feature bacterial phylum in  
458 sediment containing high concentration of CNTs. The significant differences in  
459 relative abundance of these bacterial phyla make them potential candidates to reflect  
460 the effects of MWCNTs and 2,4-DCP on sediment bacterial community.

461

462 **4. Conclusions**

463 In summary, the experimental results showed that MWCNTs could affect the  
464 potential risks of 2,4-DCP in riverine sediment. The presence of MWCNTs increased  
465 the adsorption of 2,4-DCP by sediment, thus influencing the microbial biomass  
466 carbon, enzyme activity, and bacterial community structure in sediment, especially at  
467 a MWCNT level of 5 mg/g. When the MWCNT concentration in sediment was  
468 extremely high (50 mg/g), the MWCNTs themselves had a greater impact on sediment  
469 microbial community. *Bacteroidetes*, *Planctomycetes*, and *Nitrospirae* were feature  
470 bacterial phyla to reflect the effects of MWCNTs and 2,4-DCP on sediment bacterial  
471 community. The response of microbial community may be a valuable indicator for the  
472 risk assessment of MWCNTs and coexisting pollutants in the aquatic environment.  
473 Additionally, these results could be considered when developing secure CNT  
474 applications and implementing sediment management.

475

Accepted MS

476 **Acknowledgements**

477 This work was supported by National Natural Science Foundation of China  
478 (51521006, 51579095, 51378190, 51508177, 51709101), the Program for Changjiang  
479 Scholars and Innovative Research Team in University (IRT-13R17), and the Three  
480 Gorges Follow-up Research Project (2017HXXY-05).

481

Accepted MS

482 **References**

- 483 Apul, O.G. and Karanfil, T., 2015. Adsorption of synthetic organic contaminants by  
484 carbon nanotubes: A critical review. *Water Res.* 68, 34-55.
- 485 Bello, D., Trasar-Cepeda, C., Leirós, M.C. and Gil-Sotres, F., 2013. Modification of  
486 enzymatic activity in soils of contrasting pH contaminated with  
487 2,4-dichlorophenol and 2,4,5-trichlorophenol. *Soil Biol. Biochem.* 56, 80-86.
- 488 Bishop, L., Cena, L., Orandle, M., Yanamala, N., Dahm, M.M., Birch, M.E., Evans,  
489 D.E., Kodali, V.K., Eye, T., Battelli, L., Zeidler-Erdely, P.C., Cucco, G., Bunker,  
490 K., Lupoi, J.S., Lersch, T.L., Stefaniak, A.B., Sargent, T., Afshari, A.,  
491 Schwegler-Berry, D., Friend, S., Kang, J., Siegert, K.J., Mitchell, C.A., Lowry,  
492 D.T., Kashon, M.L., Mercer, R.R., Geraci, C.L., Schubauer-Berigan, M.K.,  
493 Sargent, L.M. and Erdely, A., 2017. In vivo toxicity assessment of occupational  
494 components of the carbon nanotube life cycle to provide context to potential  
495 health effects. *ACS Nano* 11, 8849-8863.
- 496 Chen, M., Zhou, Y., Zhu, Y., Sun, Y., Zeng, G., Yang, C., Xu, P., Yan, M., Liu, Z. and  
497 Zhang, W., 2018. Toxicity of carbon nanomaterials to plants, animals and  
498 microbes: Recent progress from 2015-present. *Chemosphere* 206, 255-264.
- 499 Cheng, W., Zhang, J., Wang, Z., Wang, M. and Xie, S., 2014. Bacterial communities  
500 in sediments of a drinking water reservoir. *Ann. Microbiol.* 64, 875-878.
- 501 Chung, H., Son, Y., Yoon, T.K., Kim, S. and Kim, W., 2011. The effect of  
502 multi-walled carbon nanotubes on soil microbial activity. *Ecotox. Environ. Safe.*  
503 74, 569-575.

504 Cordero, I., Snell, H. and Bardgett, R.D., 2019. High throughput method for  
505 measuring urease activity in soil. *Soil Biol. Biochem.* 134, 72-77.

506 Curd, E.E., Martiny, J.B.H., Li, H. and Smith, T.B., 2018. Bacterial diversity is  
507 positively correlated with soil heterogeneity. *Ecosphere* 9, e02079.

508 Dallinger, A. and Horn, M.A., 2014. Agricultural soil and drilosphere as reservoirs of  
509 new and unusual assimilators of 2,4-dichlorophenol carbon. *Environ. Microbiol.*  
510 16, 84-100.

511 Deng, Q., Cheng, X., Hui, D., Zhang, Q., Li, M. and Zhang, Q., 2016. Soil microbial  
512 community and its interaction with soil carbon and nitrogen dynamics following  
513 afforestation in central China. *Sci. Total Environ.* 541, 230-237.

514 Ertürk, M.D. and Saçan, M.T., 2012. First toxicity data of chlorophenols on marine  
515 alga *Dunaliella tertiolecta*: Correlation of marine algal toxicity with  
516 hydrophobicity and interspecific toxicity relationships. *Environ. Toxicol. Chem.*  
517 31, 1113-1120.

518 Fajardo, C., Cosme, G., Nardie, M., Botías, P., García-Cantalejo, J. and Martín, M.,  
519 2019. Pb, Cd, and Zn soil contamination: Monitoring functional and structural  
520 impacts on the microbiome. *Appl. Soil. Ecol.* 135, 56-64.

521 Fan, X., Xu, J., Lavoie, M., Peijnenburg, W.J.G.M., Zhu, Y., Lu, T., Fu, Z., Zhu, T. and  
522 Qian, H., 2018. Multiwall carbon nanotubes modulate paraquat toxicity in  
523 *Arabidopsis thaliana*. *Environ. Pollut.* 233, 633-641.

524 Feng, W. and Ji, P., 2011. Enzymes immobilized on carbon nanotubes. *Biotechnol.*  
525 *Adv.* 29, 889-895.

526 Flores, C., Catita, J.A.M. and Lage, O.M., 2014. Assessment of planctomycetes cell  
527 viability after pollutants exposure. *Antonie van Leeuwenhoek* 106, 399-411.

528 Frossard, A., Gerull, L., Mutz, M. and Gessner, M.O., 2012. Disconnect of microbial  
529 structure and function: enzyme activities and bacterial communities in nascent  
530 stream corridors. *ISME J.* 6, 680-691.

531 Gao, J., Liu, L., Liu, X., Zhou, H., Huang, S. and Wang, Z., 2008. Levels and spatial  
532 distribution of chlorophenols – 2,4-Dichlorophenol, 2,4,6-trichlorophenol, and  
533 pentachlorophenol in surface water of China. *Chemosphere* 71, 1181-1187.

534 Gottschalk, F., Sonderer, T., Scholz, R.W. and Nowack, B., 2009. Modeled  
535 environmental concentrations of engineered nanomaterials (TiO<sub>2</sub>, ZnO, Ag, CNT,  
536 Fullerenes) for different regions. *Environ. Sci. Technol.* 43, 9216-9222.

537 Huang, D., Zhang, X., Zhang, C., Li, H., Li, D., Hu, Y., Yang, F. and Qi, Y., 2018.  
538 2,4-Dichlorophenol induces DNA damage through ROS accumulation and GSH  
539 depletion in goldfish *Carrasius auratus*. *Environ. Mol. Mutagen.* 59, 798-804.

540 Igbinosa, E.O., Odiayire, E.E., Chigor, V.N., Igbinosa, I.H., Emoghene, A.O.,  
541 Ekhaize, F.O., Ijehon, N.O. and Idemudia, O.G., 2013. Toxicological profile of  
542 chlorophenols and their derivatives in the environment: the public health  
543 perspective. *Sci. World J.* 2013, Article ID 460215,  
544 <https://doi.org/460210.461155/462013/460215>.

545 Jesionowski, T., Zdarta, J. and Krajewska, B., 2014. Enzyme immobilization by  
546 adsorption: a review. *Adsorption* 20, 801-821.

547 Köhler, A.R., Som, C., Helland, A. and Gottschalk, F., 2008. Studying the potential

548 release of carbon nanotubes throughout the application life cycle. *J. Clean. Prod.*  
549 16, 927-937.

550 Kerfahi, D., Tripathi, B.M., Singh, D., Kim, H., Lee, S., Lee, J. and Adams, J.M.,  
551 2015. Effects of functionalized and raw multi-walled carbon nanotubes on soil  
552 bacterial community composition. *PLOS ONE* 10, e0123042.

553 Khairy, M.A., 2013. Assessment of priority phenolic compounds in sediments from an  
554 extremely polluted coastal wetland (Lake Maryut, Egypt). *Environ. Monit. Assess.*  
555 185, 441-455.

556 Koelmans, A.A., Nowack, B. and Wiesner, M.R., 2009. Comparison of manufactured  
557 and black carbon nanoparticle concentrations in aquatic sediments. *Environ.*  
558 *Pollut.* 157, 1110-1116.

559 Koliada, A., Syzenko, G., Moseiko, V., Budzowska, L., Puchkov, K., Perederiy, V.,  
560 Gavalko, Y., Dorofeyev, A., Koshchynko, M., Tkach, S., Sineok, L., Lushchak, O.  
561 and Vaiserman, A., 2015. Association between body mass index and  
562 *Firmicutes/Bacteroidetes* ratio in an adult Ukrainian population. *BMC Microbiol.*  
563 17, 120.

564 Kragulj, M., Tričković, J., Kukovec, Á., Jović, B., Molnar, J., Rončević, S., Kónya,  
565 Z. and Dalmacija, B., 2015. Adsorption of chlorinated phenols on multiwalled  
566 carbon nanotubes. *RSC Adv.* 5, 24920-24929.

567 Liu, H.H. and Cohen, Y., 2014. Multimedia environmental distribution of engineered  
568 nanomaterials. *Environ. Sci. Technol.* 48, 3281-3292.

569 Liu, Y., Dai, Q., Jin, X., Dong, X., Peng, J., Wu, M., Liang, N., Pan, B. and Xing, B.,

570 2018. Negative impacts of biochars on urease activity: high pH, heavy metals,  
571 polycyclic aromatic hydrocarbons, or free radicals? Environ. Sci. Technol. 52,  
572 12740-12747.

573 Lozupone, C., Lladser, M.E., Knights, D., Stombaugh, J. and Knight, R., 2011.  
574 UniFrac: an effective distance metric for microbial community comparison.  
575 ISME J. 5, 169-172.

576 Mierzwa-Hersztek, M., Gondek, K. and Baran, A., 2016. Effect of poultry litter  
577 biochar on soil enzymatic activity, ecotoxicity and plant growth. Appl. Soil. Ecol.  
578 105, 144-150.

579 Myer, M.H., Henderson, W.M. and Black, M.C., 2007. Effects of multiwalled carbon  
580 nanotubes on the bioavailability and toxicity of diphenhydramine to *Pimephales*  
581 *promelas* in sediment exposures. Environ. Toxicol. Chem. 36, 320-328.

582 Orland, C., Emilson, E.J.S., Pasnik, N., Mykytczuk, N.C.S., Gunn, J.M. and  
583 Tanentzap, A.J., 2019. Microbiome functioning depends on individual and  
584 interactive effects of the environment and community structure. ISME J. 13, 1-11.

585 Price, M.N., Dehan, P.S. and Arkin, A.P., 2010. FastTree 2 – Approximately  
586 Maximum-Likelihood Trees for Large Alignments. PLOS ONE 5, e9490.

587 Qian, H., Ke, M., Qu, Q., Li, X., Du, B., Lu, T., Sun, L. and Pan, X., 2018. Ecological  
588 effects of single-walled carbon nanotubes on soil microbial communities and soil  
589 fertility. Bull. Environ. Contam. Toxicol. 101, 536-542.

590 Schnorr, J.M. and Swager, T.M., 2011. Emerging applications of carbon nanotubes.  
591 Chem. Mater. 23, 646-657.

592 Segata, N., Izard, J., Waldron, L., Gevers, D., Miropolsky, L., Garrett, W.S. and  
593 Huttenhower, C., 2011. Metagenomic biomarker discovery and explanation.  
594 *Genome Biol.* 12, R60.

595 Shen, M., Zhang, Y., Tian, Y. and Zeng, G., 2018. Recent advances in research on  
596 cyclic volatile methylsiloxanes in sediment, soil and biosolid: a review. *Chem.*  
597 *Ecol.* 34, 675-695.

598 Shrestha, B., Acosta-Martinez, V., Cox, S.B., Green, M.J., Li, S. and Cañas-Carrell,  
599 J.E., 2013. An evaluation of the impact of multiwalled carbon nanotubes on soil  
600 microbial community structure and functioning. *J. Hazard. Mater.* 261, 188-197.

601 Smith, S.C. and Rodrigues, D.F., 2015. Carbon-based nanomaterials for removal of  
602 chemical and biological contaminants from water. A review of mechanisms and  
603 applications. *Carbon* 91, 122-143.

604 Song, B., Xu, P., Zeng, G., Gong, J., Zhang, P., Feng, H., Liu, Y. and Ren, X., 2018a.  
605 Carbon nanotube-based environmental technologies: the adopted properties,  
606 primary mechanisms and challenges. *Rev. Environ. Sci. Biotechnol.* 17, 571-590.

607 Song, B., Zeng, G., Gong, J., Zhang, P., Deng, J., Deng, C., Yan, J., Xu, P., Lai, C.,  
608 Zhang, C. and Cheng, M., 2017a. Effect of multi-walled carbon nanotubes on  
609 phytotoxicity of sediments contaminated by phenanthrene and cadmium.  
610 *Chemosphere* 172, 449-458.

611 Song, B., Chen, M., Ye, S., Xu, P., Zeng, G., Gong, J., Li, J., Zhang, P. and Cao, W.,  
612 2019. Effects of multi-walled carbon nanotubes on metabolic function of the  
613 microbial community in riverine sediment contaminated with phenanthrene.

614 Carbon 144, 1-7.

615 Song, B., Zeng, G., Gong, J., Liang, J., Xu, P., Liu, Z., Zhang, Y., Zhang, C., Cheng,  
616 M., Liu, Y., Ye, S., Yi, H. and Ren, X., 2017b. Evaluation methods for assessing  
617 effectiveness of in situ remediation of soil and sediment contaminated with  
618 organic pollutants and heavy metals. *Environ. Int.* 105, 43-55.

619 Song, B., Xu, P., Zeng, G., Gong, J., Wang, X., Yan, J., Wang, S., Zhang, P., Cao, W.  
620 and Ye, S., 2018b. Modeling the transport of sodium dodecyl benzene sulfonate  
621 in riverine sediment in the presence of multi-walled carbon nanotubes. *Water Res.*  
622 129, 20-28.

623 Tamez Ramírez, M.d.S. and Vega-Cantú, Y.I., 2019. Nanotechnology learning through  
624 product development. *Int. J. Interact. Des. Manuf.* 13, 1013-1027.

625 Tan, X., Liu, Y., Yan, K., Wang, Z., Lu, G., He, Y. and He, W., 2017a. Differences in  
626 the response of soil dehydrogenase activity to Cd contamination are determined  
627 by the different substrates used for its determination. *Chemosphere* 169, 324-332.

628 Tan, X., Wang, Z., Lu, G., He, W., Wei, G., Huang, F., Xu, X. and Shen, W., 2017b.  
629 Kinetics of soil dehydrogenase in response to exogenous Cd toxicity. *J. Hazard.*  
630 *Mater.* 329, 299-309.

631 Wang, F., Haftka, J.J.H., Sinnige, T.L., Hermens, J.L.M. and Chen, W., 2014.  
632 Adsorption of polar, nonpolar, and substituted aromatics to colloidal graphene  
633 oxide nanoparticles. *Environ. Pollut.* 186, 226-233.

634 Wang, Q., Garrity, G.M., Tiedje, J.M. and Cole, J.R., 2007. Naïve Bayesian Classifier  
635 for Rapid Assignment of rRNA Sequences into the New Bacterial Taxonomy.

636 Appl. Environ. Microb. 73, 5261-5267.

637 Wolińska, A., Kuźniar, A., Zielenkiewicz, U., Izak, D., Szafranek-Nakonieczna, A.,  
638 Banach, A. and Błaszczuk, M., 2017. Bacteroidetes as a sensitive biological  
639 indicator of agricultural soil usage revealed by a culture-independent approach.  
640 Appl. Soil. Ecol. 119, 128-137.

641 Wu, H.Y., Xu, H.X., Hong, Y.B., Zhang, J.F. and Wu, J.C., 2011. The use of  
642 biomarkers in the antioxidant responses of *Daphnia magna* to the acute and  
643 chronic exposure to no. 20 diesel oil and 2,4-dichlorophenol. J. Chem. Spec.  
644 Bioavailab. 23, 80-87.

645 Xie, Y., Wang, J., Wu, Y., Ren, C., Song, C., Yang, Y., Yu, H., Giesy, J.P. and Zhang,  
646 X., 2016. Using in situ bacterial communities to monitor contaminants in river  
647 sediments. Environ. Pollut. 212, 348-357.

648 Zhai, P., Isaacs, J.A. and Eckman, M.J., 2016. Net energy benefits of carbon  
649 nanotube applications. Applied Energy 173, 624-634.

650 Zhang, J., Yang, Y., Zhao, L., Li, Y., Xie, S. and Liu, Y., 2015. Distribution of  
651 sediment bacterial and archaeal communities in plateau freshwater lakes. Appl.  
652 Microbiol. Biot. 99, 3291-3302.

653 Zhang, J., Mao, F., Loh, K.C., Gin, K.Y.H., Dai, Y. and Tong, Y.W., 2018. Evaluating  
654 the effects of activated carbon on methane generation and the fate of antibiotic  
655 resistant genes and class I integrons during anaerobic digestion of solid organic  
656 wastes. Bioresource Technol. 249, 729-736.

657 Zhou, M., Zhang, J. and Sun, C., 2017. Occurrence, ecological and human health risks,

658 and seasonal variations of phenolic compounds in surface water and sediment of  
659 a potential polluted river basin in China. *Int. J. Env. Res. Pub. He.* 14, 1140.

660 Zhou, W., Shan, J., Jiang, B., Wang, L., Feng, J., Guo, H. and Ji, R., 2013. Inhibitory  
661 effects of carbon nanotubes on the degradation of  $^{14}\text{C}$ -2,4-dichlorophenol in soil.  
662 *Chemosphere* 90, 527-534.

663 Zhu, J., Zhang, J., Li, Q., Han, T., Xie, J., Hu, Y. and Chai, L., 2013. Phylogenetic  
664 analysis of bacterial community composition in sediment contaminated with  
665 multiple heavy metals from the Xiangjiang River in China. *Mar. Pollut. Bull.* 70,  
666 134-139.

Accepted MS

**Table 1**

Parameters of the isotherm models for 2,4-DCP adsorption.

Concentration of MWCNTs in sediment (mg/g)	Langmuir model			Freundlich model		
	$q_m$ (mg/g)	$K_L$ (L/mg)	$R^2$	$K_F$ (mg/g·(mg/L) <sup>-1/n</sup> )	$1/n$	$R^2$
0	0.541	0.00897	0.986	0.00918	0.737	0.980
5	1.00	0.0108	0.978	0.0227	0.696	0.988
10	1.18	0.0193	0.970	0.0546	0.601	0.994
15	1.44	0.0310	0.989	0.106	0.540	0.997
Pure MWCNTs	47.6	0.163	0.944	15.5	0.261	0.997

Accepted MS

**Figure 1**

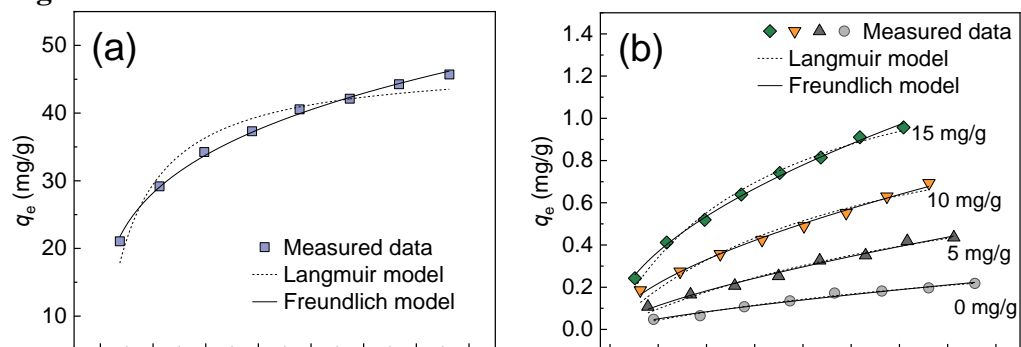


**Fig. 1.** Isotherms of 2,4-DCP adsorption by MWCNTs (a) and sediments with different MWCNT concentrations (b).

Accepted MS

Figure 2

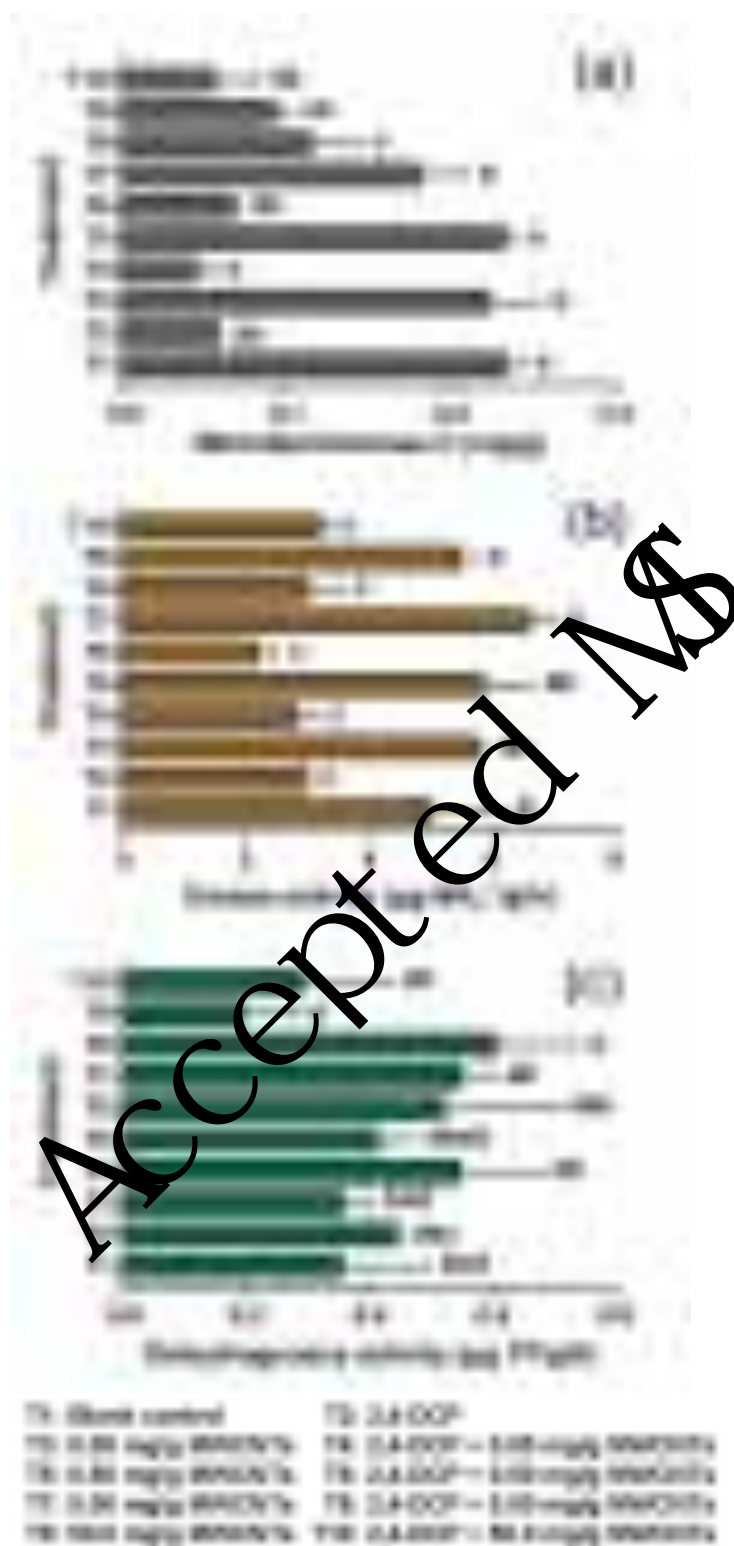


**Fig. 2.** Microbial biomass carbon (a), urease activity (b), and dehydrogenase activity (c) of the sediments from different treatments. Different letters denote statistically significant differences ( $P < 0.05$ ) between groups.

**Figure 3**



**Fig. 3.** Bacterial community structure in sediments from different treatments at phylum (a) and class (b) level.

Figure 4

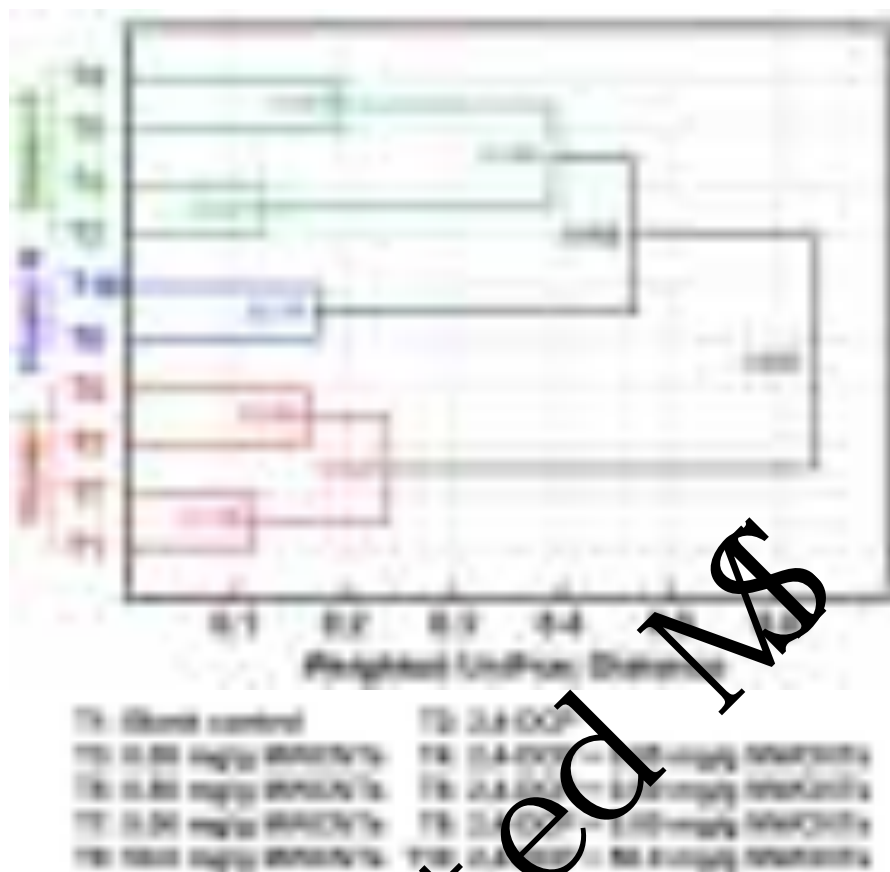
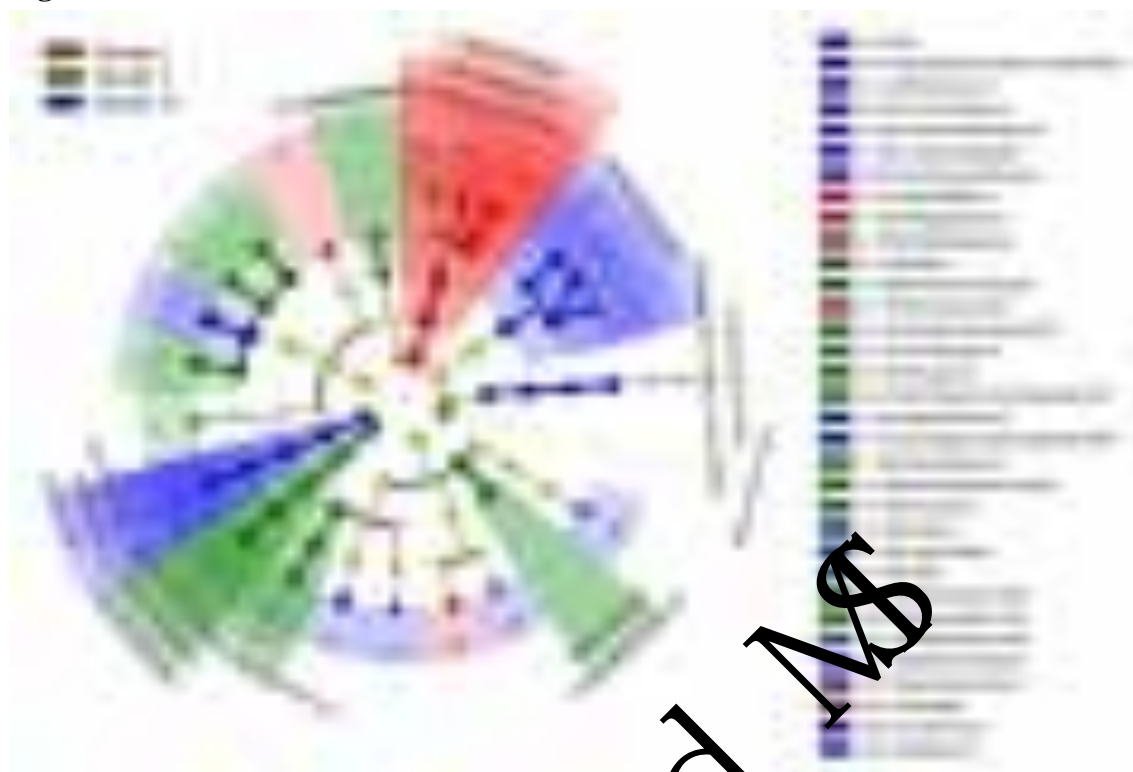


Fig. 4. Phylogenetic analysis of the bacterial communities in different treatments based on weighted UniFrac distance.

**Figure 5**



**Fig. 5.** Cladogram plotted from LEfSe analysis showing the significant differences ( $P < 0.05$ ) in relative abundance of bacterial taxon among different clusters based on the analysis of weighted UniFrac distance. Different colors (red, green, and blue) indicate different clusters. The colored dots from inner to outer represent phylum, class, order, family, and genus levels, and the dot size suggests the relative abundance of bacterial taxon. The taxon with significant difference in relative abundance among clusters is shown by the dot colored in red, green, or blue, while yellow dot represents that the relative abundance of corresponding taxon is not significantly different among different clusters. The colored shadows indicate the trends of significantly different taxa. The names of significant different taxa at family and genus levels are listed on the right. Only taxa with a logarithmic LDA score more than 3.5 are shown on the cladogram.

## Electronic Supplementary Material for

### **Influence of multi-walled carbon nanotubes on the microbial biomass, enzyme activity, and bacterial community structure in 2,4-dichlorophenol-contaminated sediment**

Biao Song<sup>a,b</sup>, Jilai Gong<sup>a,b</sup>, Wangwang Tang<sup>a,b</sup>, Guangming Zeng<sup>a,b,\*</sup>, Ming Chen<sup>a,b</sup>, Piao Xu<sup>a,b</sup>,  
Maocai Shen<sup>a,b</sup>, Shujing Ye<sup>a,b</sup>, Haopeng Feng<sup>a,b</sup>, Chengyun Zhou<sup>a,b</sup>, Yang Yang<sup>a,b</sup>

<sup>a</sup> College of Environmental Science and Engineering, Hunan University, Changsha 410082, PR China

<sup>b</sup> Key Laboratory of Environmental Biology and Pollution Control (Hunan University), Ministry of Education, Changsha 410082, PR China

\* Corresponding author at: College of Environmental Science and Engineering, Hunan University, Changsha 410082, PR China.

E-mail addresses: [zgming@hnu.edu.cn](mailto:zgming@hnu.edu.cn) (G. Zeng).

### Calculation of adsorption amount

The adsorption amount  $q_e$  (mg/g) is calculated by the following equation:

$$q_e = \frac{(c_0 - c_e) \times V}{m}$$

where  $c_0$  (mg/L) is the initial concentration of 2,4-DCP,  $c_e$  (mg/L) is the equilibrium concentration of 2,4-DCP,  $V$  (L) is the volume of solution, and  $m$  (g) is the weight of adsorbent.

### Langmuir and Freundlich isotherm models

The Langmuir and Freundlich isotherm models are given by the following equations:

Langmuir model:  $q_e = \frac{q_m K_L c_e}{1 + K_L c_e}$

Freundlich model:  $q_e = K_F c_e^{\frac{1}{n}}$

where  $q_e$  (mg/g) is the amount of adsorbed 2,4-DCP at equilibrium,  $q_m$  (mg/g) is the maximum adsorption capacity,  $K_L$  (L/mg) is the Langmuir constant,  $c_e$  (mg/L) is the equilibrium concentration of 2,4-DCP,  $K_F$  (mg/g(mg/L)<sup>-1/n</sup>) and  $n$  (dimensionless) are Freundlich constants.

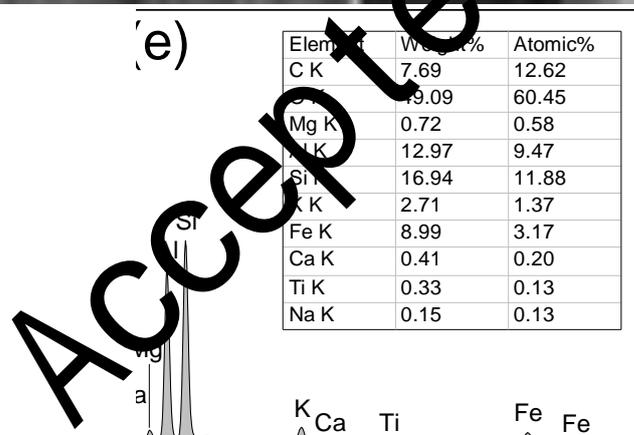


**Fig. S1.** SEM images of the used MWCNTs (a and b) and sediment (c and d), and EDS analysis of the sediment (e).





**Fig. S3.** Relative abundance of three feature bacterial phyla in cluster I (a), cluster II (b), and cluster III (c) identified from LEfSe analysis. The means and medians in each cluster are shown with straight lines and dotted lines, respectively.

**Table S1**

Experimental design for studying the effects of MWCNTs on microbial community in riverine sediment contaminated with 2,4-DCP.

Treatment	Components		
Treatment 1 (T1)	Sediment	–	–
Treatment 2 (T2)	Sediment	2,4-DCP (30 mg/kg)	–
Treatment 3 (T3)	Sediment	–	MWCNTs (0.05 mg/g)
Treatment 4 (T4)	Sediment	2,4-DCP (30 mg/kg)	MWCNTs (0.05 mg/g)
Treatment 5 (T5)	Sediment	–	MWCNTs (0.50 mg/g)
Treatment 6 (T6)	Sediment	2,4-DCP (30 mg/kg)	MWCNTs (0.50 mg/g)
Treatment 7 (T7)	Sediment	–	MWCNTs (5.00 mg/g)
Treatment 8 (T8)	Sediment	2,4-DCP (30 mg/kg)	MWCNTs (5.00 mg/g)
Treatment 9 (T9)	Sediment	–	MWCNTs (50.0 mg/g)
Treatment 10 (T10)	Sediment	2,4-DCP (30 mg/kg)	MWCNTs (50.0 mg/g)

Accepted MS

**Table S2**

Estimation of biota-sediment accumulation factor (BSAF) for 2,4-DCP in sediments with different concentration of MWCNTs.

Concentration of MWCNTs in sediment (mg/g)	$K_d$ (L/kg) <sup>a</sup>	BSAF <sup>b</sup>
0	2.6	31.8
5	5.4	15.3
10	8.3	10.0
15	12.6	6.6

<sup>a</sup> Equilibrium partition coefficient ( $K_d$ ) was calculated from the adsorption isotherms.

<sup>b</sup> BSAF was calculated using  $\log K_{ow} = 3.08$ ,  $\log BCF = 0.85 \log K_{ow} - 0.70$ , and  $BSAF = BCF/K_d$  (Jiao et al. 2014, Meng et al. 2018).  $K_{ow}$ : octanol-water partitioning coefficient, BCF: bioconcentration factor.

Accepted MS

**Table S3**

P-values from two-way ANOVA for the effects of MWCNTs and 2,4-DCP on the microbial biomass carbon, urease activity, and dehydrogenase activity.

	Microbial biomass C	Urease activity	Dehydrogenase activity
MWCNTs	0.001	0.248	0.020
2,4-DCP	< 0.001	< 0.001	0.053
MWCNTs × 2,4-DCP	0.001	0.148	0.933

Accepted MS

**Table S4**

Alpha diversity index for different treatments.

Treatment	Chao1 index <sup>a</sup>	Shannon index <sup>b</sup>
T1	3620.56	4.36
T2	4447.10	5.47
T3	3824.19	4.00
T4	4736.10	5.30
T5	4384.86	4.50
T6	4114.36	5.27
T7	3740.88	4.45
T8	4082.39	5.30
T9	3534.78	5.00
T10	3421.11	5.11

<sup>a</sup> Chao1 index indicates the number of OTU species.

<sup>b</sup> Shannon index reflects the species diversity that takes into account both the species richness and evenness (Niu et al. 2020).

Accepted MS

## References

Jiao, W., Wang, T., Lu, Y., Chen, W. and He, Y., 2014. Ecological risks of polycyclic aromatic hydrocarbons found in coastal sediments along the northern shores of the Bohai Sea (China). *Chemistry and Ecology* 30(6), 501-512.

Meng, W.K., Liu, L., Wang, X., Zhao, R.S., Wang, M.L. and Lin, J.M., 2018. Polyphenylene core-conjugated microporous polymer coating for highly sensitive solid-phase microextraction of polar phenol compounds in water samples. *Analytica Chimica Acta* 1015, 27-34.

Niu, H., Leng, Y., Ran, S., Ameer, M., Du, D., Sun, J., Chen, K. and Hong, S., 2020. Toxicity of soil labile aluminum fractions and aluminum species in soil water extracts on the rhizosphere bacterial community of tall fescue. *Ecotoxicology and Environmental Safety* 187, 109828.

Accepted MS